

# Vehicle Velocity Estimation using Modular Nonlinear Observers\*

Lars Imsland\* Tor A. Johansen<sup>\*,†</sup> Thor I. Fossen<sup>\*,†</sup>  
\*SINTEF ICT, Applied Cybernetics  
N-7465 Trondheim, Norway

Jens C. Kalkkuhl<sup>‡</sup> Avshalom Suissa<sup>‡</sup>  
<sup>‡</sup>DaimlerChrysler Research and Technology  
70456 Stuttgart, Germany

**Abstract**—Nonlinear observers for estimation of lateral and longitudinal velocity of automotive vehicles are proposed, based on acceleration and yaw rate measurements in addition to wheel speed and steering angle. The observer for lateral velocity uses a tyre-road friction model. Exponential stability of the observers are shown. A structural assumption on the friction model is discussed. The observer structure is validated using experimental data from cars.

## I. INTRODUCTION

Feedback control systems for active safety in automotive applications have over the last years entered production cars. Many of these systems have in common that the control action depend on information about vehicle velocity, or sideslip. However, the velocity is seldom measured directly, and must therefore be inferred from other measurements such as wheel speeds and acceleration measurements.

The main goal of this work is to derive observers for vehicle velocity with stability guarantees. Towards this goal, we propose a cascaded observer structure, and prove stability of the observers under certain conditions. Nonlinear observers are used for taking the nonlinear dynamics (mainly due to highly non-linear friction forces) into account, and to obtain simple designs with few tuning knobs (as opposed to extended Kalman filter designs). Another significant advantage of the proposed approach is that the Riccati equation is avoided, such that the observer can be implemented efficiently in a low-cost embedded computer unit.

Earlier works on observers for estimation of lateral velocity are mainly based on linear or quasi-linear techniques, e.g. [1–4]. A nonlinear observer linearizing the observer error dynamics have been proposed in [5], [6]. The same type of observer, in addition to an observer based on forcing the dynamics of the nonlinear estimation error to the dynamics of a linear reference system, are investigated in [7]. The problem formulation there assumes that the longitudinal wheel forces are known, as the observer implemented in ESP also does [8]. In our work, we do not make this assumption, as such information is not always available. Nevertheless, if this information is available, it might be natural to use it in the first module of our modular approach (estimation of longitudinal velocity).

The Extended Kalman-filter is used for estimating vehicle velocity and tyre forces in [9], [10], thus without the explicit use of friction models. A similar, but simpler, approach is also suggested in [4]. An Extended Kalman-filter based on a tyre-road friction models that also included estimation of the adhesion coefficient and road inclination angle is

\*This research is supported by the European Commission STREP project CEMACS, contract 004175.

<sup>†</sup>Also affiliated with Department of Engineering Cybernetics, Norwegian University of Science and Technology, N-7491 Trondheim, Norway.

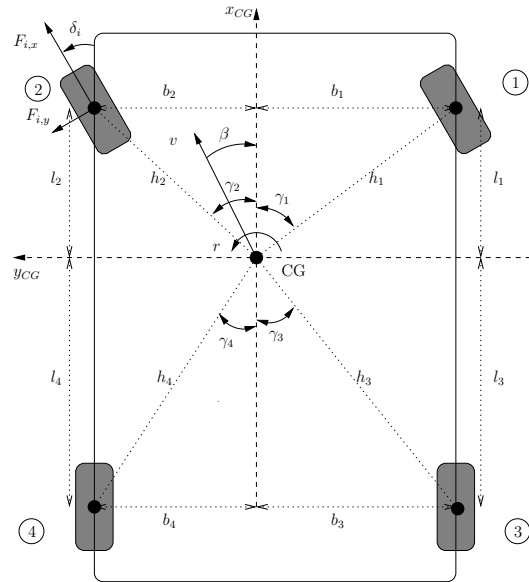


Fig. 1. Horizontal axis systems, geometric definitions, wheel forces, speed, slip angle and yaw rate.

suggested in [11]. [12] considers the use of an Extended Kalman-filter, based on a nonlinear tyre-friction model, that also includes estimation of cornering stiffness. The strategy proposed in [13] combines dynamic and kinematic models of the vehicle with numerical bandlimited integration of the equations to provide a side-slip estimate. In [14] side-slip angle is estimated along with yaw rate in an approach that has similarities with the one considered herein, while using fewer measurements. The approach in [14] is validated using experimental data, but there are no stability proofs.

## II. VEHICLE MODELING

### A. Rigid body dynamics

The geometry of the vehicle and the involved coordinate systems are illustrated in Figure 1. The vehicle velocity is defined in a coordinate system with the origin at the vehicle center of gravity (CG, assumed constant), with  $x$ -axis pointing forward and  $y$ -axis to the left. There is a coordinate system in the centre of each wheel, aligned with the orientation of the wheel. The distance from CG to each wheel center is denoted  $h_i$ , with  $i$  being wheel index. Together with the angles  $\gamma_i$ , this defines the vehicle geometry. We will assume that we can consider the vehicle a rigid body, for which the rigid body dynamics (with respect to the CG coordinate system) can be written

$$M\dot{\nu} + C(\nu)\nu = \tau \quad (1)$$

where  $\nu$  is a vector containing the body generalized velocities. The matrices  $\mathbf{M}$  and  $\mathbf{C}$  are the inertia matrix, and Coriolis and centripetal matrix, respectively. The vector  $\tau$  consists of forces and torques on the vehicle, mainly friction forces acting via the wheels, but also gravitational, weather (wind), and aerodynamic (air resistance) forces are at work.

By making the following assumptions,

- Only include motion in the horizontal plane (ignore dynamics related to vertical motion, including roll and pitch).
- The effect of caster and camber is ignored
- Only tyre friction and gravitational forces are affecting vehicle motion

the vehicle dynamics are described by longitudinal velocity  $v_x$ , lateral velocity  $v_y$  and yaw rate  $r$ , resulting in the “two-track model” [6], with

$$\mathbf{M} = \begin{pmatrix} m & 0 & 0 \\ 0 & m & 0 \\ 0 & 0 & J_z \end{pmatrix}, \quad \mathbf{C}(\nu) = \begin{pmatrix} 0 & -mr & 0 \\ mr & 0 & 0 \\ 0 & 0 & 0 \end{pmatrix}.$$

The generalized forces  $\tau = (f_x, f_y, m_z)^\top$  are forces and torque generated by friction between the wheels and the ground, and gravitational forces induced by road inclination ( $\theta_R$ ) and road bank angle ( $\phi_R$ ):

$$\tau = \begin{pmatrix} f_x \\ f_y \\ m_z \end{pmatrix} = \sum_i \begin{pmatrix} \mathbf{I}_{2 \times 2} \\ \mathbf{g}_i^\top \end{pmatrix} \mathbf{R}(\delta_i) \mathbf{F}_i + \begin{pmatrix} mg \sin \phi_R \\ -mg \sin \theta_R \\ 0 \end{pmatrix}.$$

The friction forces  $\mathbf{F}_i$  working at each wheel (see Figure 1) are functions of vehicle velocity, see the next section. They are transformed from the wheel coordinate systems to CG:

- The forces generated by the tyres in body-fixed coordinates for each wheel  $i$ , is:

$$\mathbf{f}_i = (f_{i,x}, f_{i,y})^\top = \mathbf{R}(\delta_i) \mathbf{F}_i$$

where  $\mathbf{F}_i = (F_{i,x}, F_{i,y})^\top$  are the forces acting on the wheel in the wheel-fixed coordinate system. The rotation matrix induced by the steering angle  $\delta_i$  is

$$\mathbf{R}(\delta_i) = \begin{pmatrix} \cos \delta_i & -\sin \delta_i \\ \sin \delta_i & \cos \delta_i \end{pmatrix}.$$

- For the torque, it is convenient to define the geometry vector  $\mathbf{g}_i = (-h_i \sin \psi_i, h_i \cos \psi_i)^\top$  transpose where the angles  $\psi_i$  are introduced to get a uniform representation,  $\psi_1 = -\gamma_1$ ,  $\psi_2 = \gamma_2$ ,  $\psi_3 = \pi + \gamma_3$  and  $\psi_4 = \pi - \gamma_4$ . The generated torque about the vertical axis through the CG is then for each wheel

$$m_{i,z} = \mathbf{g}_i^\top \mathbf{f}_i. \quad (2)$$

### B. Friction models

In most friction models, the friction forces are functions of tyre slips, which are measures of the relative difference in vehicle and tyre velocity. One definition for the longitudinal and lateral tyre slips are

$$\lambda_{i,x} = \frac{\omega_i R_{dyn} - V_{i,x}}{V_{i,x}}, \quad \lambda_{i,y} = \sin \alpha_i,$$

where  $\omega_i$  is the wheel angular velocity,  $R_{dyn}$  is the dynamic wheel radius, the tyre slip angles are calculated as  $\alpha_i =$

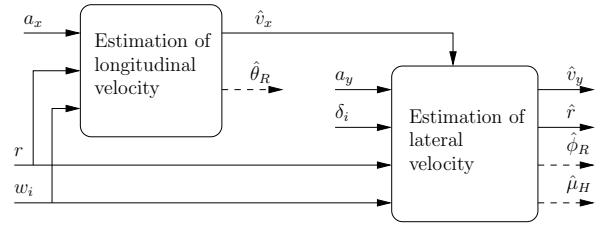


Fig. 2. Modular observer structure

$\delta_i - \arctan \frac{v_{i,y}}{v_{i,x}}$ , and  $V_{i,x}$  is the velocity in  $x$ -direction in the wheel coordinate system,  $V_{i,x} = \sqrt{v_{i,x}^2 + v_{i,y}^2} \cos \alpha_i$ . The longitudinal and lateral velocities of the wheel center in the body-fixed coordinate system are  $v_{i,x} = v_x \pm rb_i$  and  $v_{i,y} = v_y \pm rb_i$ . For the tyre slip angles to be well defined, we assume that

*Assumption 1:*  $v_{i,x} > 0$  for  $i = 1, \dots, 4$ .

The tyre slips depend on the vehicle states and the time-varying, measured parameters  $\omega_i$  and  $\delta_i$ . We will use the two notations  $\mathbf{F}_i = \mathbf{F}_i(\lambda_{i,x}, \lambda_{i,y}) = \mathbf{F}_i(\mathbf{x}, \boldsymbol{\theta})$  interchangeably, depending on context. Since the friction model is mainly used in the estimation of lateral velocity where  $\mathbf{x} = (v_y, r)^\top$ , we let  $v_x$  be part of the time-varying parameter vector  $\boldsymbol{\theta} = (\delta_1, \dots, \delta_4, \omega_1, \dots, \omega_4, v_x)$ .

The following assumption is made on the friction model:

*Assumption 2:* There exist a positive constant  $c_1$  and sets  $\Theta$  and  $X(\boldsymbol{\theta})$ , such that for all  $\boldsymbol{\theta} \in \Theta$ ,  $X(\boldsymbol{\theta})$  is convex, the friction model is continuously differentiable wrt  $\mathbf{x}$  with  $\|\frac{\partial \mathbf{F}}{\partial \mathbf{x}}\|$  bounded on  $X(\boldsymbol{\theta}) \times \Theta$ , and

$$\sum_i \frac{\partial F_{i,y}(\mathbf{x}, \boldsymbol{\theta})}{\partial v_y} \cos \delta_i + \frac{\partial F_{i,x}(\mathbf{x}, \boldsymbol{\theta})}{\partial v_y} \sin \delta_i < -c_1, \quad (3)$$

for all  $\boldsymbol{\theta} \in \Theta$ ,  $\mathbf{x} \in X(\boldsymbol{\theta})$ .

This Assumption is discussed in Section V.

### III. OBSERVER STRUCTURE

The overall observer structure is illustrated in Figure 2. The first observer use information of (mainly) wheel speed in addition to yaw rate and longitudinal acceleration to estimate longitudinal velocity. Thereafter, this estimate is used together with measurements of lateral acceleration, yaw rate, wheel speeds, and wheel steering angle to estimate lateral velocity. In this work, the road bank and inclination angle ( $\phi_R$  and  $\theta_R$ ) are ignored (assumed to be zero). The maximal friction coefficient  $\mu_H$  might also be estimated, or be obtained from other sources (which is assumed herein). The measurements used are summarized in the Table I. Acceleration and yaw rate sensors are assumed placed in CG. The acceleration measurements have bias removed.

TABLE I  
MEASUREMENTS

Measurement	Explanation
$a_x, a_y$	Long./lat. corrected acceleration measurements
$r$	yaw rate
$\omega_i$	Rotational speed wheel $i$
$\delta_i$	Steering angle wheel $i$

The model described in Section II will be simplified for each of the observers: For estimating longitudinal velocity, we will ignore lateral ( $v_y$  and  $r$ ) dynamics, and when estimating lateral dynamics, we assume that  $v_x$  is known (thus using only two dynamic states). The main motivation for structuring the observer in this way, is that it results in a modular design with few tuning knobs.

This observer structure is cascaded, since there are no feedback loops between the observers. A simple stability result for this cascade is given in Section IV-C.

#### IV. NONLINEAR OBSERVERS FOR VELOCITY ESTIMATION

##### A. Estimation of longitudinal velocity

In estimation of longitudinal velocity, we will use a model including forward velocity only, with acceleration as input

$$\dot{v}_x = a_x. \quad (4)$$

The measurements are the wheel rotational speeds  $\omega_i$ , which are transformed to  $v_x$ , longitudinal velocity of CG, using  $v_{i,x} = v_x \pm r b_i$  and  $v_{i,x} = R_{dyn} \omega_i \cos \delta_i$  (assuming zero slip). The transformed measurement from wheel speed  $i$  is denoted  $v_{x,i}$ . Using this, we propose the following observer:

$$\dot{\hat{v}}_x = a_x + \sum_i K_i(a_x)(v_{x,i} - \hat{v}_x), \quad (5)$$

The observer gains  $K_i$  depends on the acceleration measurement, to reflect when the wheel speed measurements are good estimates of velocity.

- **Large positive  $a_x$ :** Large gain on non-driven wheels, small gain on driven wheels.
- **Small positive  $a_x$ :** Very large gain on non-driven wheels, large gain on driven wheels.
- **Small negative  $a_x$ :** Large gain on non-driven wheels, large gain on driven wheels.
- **Large negative  $a_x$ :** Small gain on non-driven wheels, small gain on driven wheel.

In [6], similar rules are used to construct a Kalman filter and a fuzzy logic estimator for vehicle velocity. Other measurements (such as flags for ABS-system, brake assistant, etc.) that provide information on validity of the zero slip assumption can also be used.

Simple outlier detection is used to avoid that blocking/spinning affect the velocity estimate.

Assuming  $v_{x,i} = v_x$  (which requires that the lateral and longitudinal slip is zero, or known), the observer is uniformly globally exponentially stable, since the gains are positive (proof is trivial, and hence omitted). Viewing the effect of slips (and missing Coriolis term) as a time-varying bounded disturbance, it is easy to show that the error dynamics are uniformly ultimately bounded [15], where the size of the ‘‘ultimate bound’’ depends on the bound on the disturbance.

##### B. Estimation of lateral velocity

Assuming (for now) the longitudinal velocity  $v_x$  known, the model we use for estimation of lateral velocity is

$$\dot{v}_y = -v_x r + a_y \quad (6a)$$

$$\dot{r} = \frac{1}{J_z} \sum_i \mathbf{g}_i^T \mathbf{R}(\delta_i) \mathbf{F}_i. \quad (6b)$$

Based on this model, we propose the following observer:

$$\dot{\hat{v}}_y = -v_x \hat{r} + a_y - K_{v_y} \left( m a_y - \sum_i [0 \ 1] \mathbf{R}(\delta_i) \hat{\mathbf{F}}_i \right) \quad (7a)$$

$$\dot{\hat{r}} = \frac{1}{J_z} \sum_i \mathbf{g}_i^T \mathbf{R}(\delta_i) \hat{\mathbf{F}}_i + K_r (r - \hat{r}) \quad (7b)$$

where  $\hat{\mathbf{F}}_i = \mathbf{F}_i(\hat{\mathbf{x}}, \boldsymbol{\theta})$  are the friction forces calculated on basis of estimates  $\hat{\mathbf{x}} = (\hat{v}_y, \hat{r})^T$ .

Define  $h(\mathbf{x}, \boldsymbol{\theta}) = \sum_i [0 \ 1] \mathbf{R}(\delta_i) \mathbf{F}_i(\mathbf{x}, \boldsymbol{\theta})$ , and the error variables  $\tilde{v}_y = v_y - \hat{v}_y$  and  $\tilde{r} = r - \hat{r}$ , and  $\tilde{\mathbf{x}} = (\tilde{v}_y, \tilde{r})$ . The following result regarding the friction forces holds due to Assumption 2:

*Lemma 1:* There exist positive constants  $c_i$ ,  $i = 1, \dots, 4$  such that for all  $\mathbf{x}, \hat{\mathbf{x}} \in X(\boldsymbol{\theta})$ ,  $\boldsymbol{\theta} \in \Theta$ , the following holds:

$$\tilde{v}_y \sum_i [0 \ 1] \mathbf{R}(\delta_i) (\mathbf{F}_i - \hat{\mathbf{F}}_i) \leq -c_1 \tilde{v}_y^2 + c_2 |\tilde{r}| |\tilde{v}_y| \quad (8a)$$

$$\frac{1}{J_z} \sum_i \mathbf{g}_i^T \mathbf{R}(\delta_i) (\mathbf{F}_i - \hat{\mathbf{F}}_i) \leq c_3 |\tilde{v}_y| + c_4 |\tilde{r}| \quad (8b)$$

*Proof:* From the Mean Value Theorem,

$$h(\mathbf{x}, \boldsymbol{\theta}) - h(\hat{\mathbf{x}}, \boldsymbol{\theta}) = \frac{\partial h(\mathbf{x}', \boldsymbol{\theta})}{\partial v_y} \tilde{v}_y + \frac{\partial h(\mathbf{x}', \boldsymbol{\theta})}{\partial r} \tilde{r}$$

where  $\mathbf{x}'$  is some point on the line segment between  $\mathbf{x}$  and  $\hat{\mathbf{x}}$ . Multiplying this with  $\tilde{v}_y$ , we get

$$\begin{aligned} \tilde{v}_y \sum_i [0 \ 1] \mathbf{R}(\delta_i) (\mathbf{F}_i - \hat{\mathbf{F}}_i) &= \\ \sum_i \left( \cos \delta_i \frac{\partial F_{i,y}(\mathbf{x}', \boldsymbol{\theta})}{\partial v_y} + \sin \delta_i \frac{\partial F_{i,x}(\mathbf{x}', \boldsymbol{\theta})}{\partial v_y} \right) \tilde{v}_y^2 &+ \\ \sum_i \left( \cos \delta_i \frac{\partial F_{i,y}(\mathbf{x}', \boldsymbol{\theta})}{\partial r} + \sin \delta_i \frac{\partial F_{i,x}(\mathbf{x}', \boldsymbol{\theta})}{\partial r} \right) \tilde{r} \tilde{v}_y. \end{aligned}$$

From Assumption 2, we arrive at (8a). From [15, Lemma 3.1], (8b) holds on  $X(\boldsymbol{\theta})$  since from Assumption 2,  $\mathbf{F}$  has continuous and bounded partial derivatives. ■

We will also make use of the following fact:

*Fact 1:* By completing the squares,

$$-a\xi_1^2 + b|\xi_1||\xi_2| = \frac{b^2}{4a}\xi_2^2 - \left( \sqrt{a}|\xi_1| - \frac{b}{2\sqrt{a}}|\xi_2| \right)^2$$

Define the set  $X_s(\rho; \boldsymbol{\theta}) = \{\mathbf{x} : B(\mathbf{x}, \rho) \subset X(\boldsymbol{\theta})\} \subset X(\boldsymbol{\theta})$  where  $B(\mathbf{x}, \rho) := \{\mathbf{z} : \|\mathbf{z} - \mathbf{x}\| \leq \rho\}$  is the ball of radius  $\rho$  around  $\mathbf{x}$ .

*Theorem 1:* Assume that  $\rho$  and  $\Theta$  are such that  $x(t) \in X_s(\rho; \boldsymbol{\theta})$ ,  $\forall t > 0$ . Let the observer gains be chosen such that

$$K_{v_y} > 0 \quad (9)$$

$$K_r > k_r + c_4 + \frac{(\bar{v}_x + K_{v_y} c_2 + c_3)^2}{2K_{v_y} c_1} \quad (10)$$

where  $\bar{v}_x$  is an upper bound on  $v_x$ , and  $k_r > 0$  is a positive constant. Then, if  $\|\tilde{\mathbf{x}}(0)\| \leq \rho$ , the state  $\hat{\mathbf{x}}(t)$  of the observer (7) converges to the state  $\mathbf{x}(t)$  of the system (6), and the origin of the observer error dynamics is uniformly exponentially stable.

*Proof:* The observer error dynamics are

$$\dot{\tilde{v}}_y = -v_x \tilde{r} + K_{v_y} \sum_i [0 \ 1] \mathbf{R}(\delta_i) (\mathbf{F}_i - \hat{\mathbf{F}}_i) \quad (11a)$$

$$\dot{\tilde{r}} = \frac{1}{J_z} \sum_i \mathbf{g}_i^T \mathbf{R}(\delta_i) (\mathbf{F}_i - \hat{\mathbf{F}}_i) - K_r \tilde{r}. \quad (11b)$$

Define the Lyapunov function candidate  $V(\tilde{\mathbf{x}}) = \frac{1}{2}(\tilde{v}_y^2 + \tilde{r}^2)$ . The time derivative along the trajectories of (11) is

$$\begin{aligned} \dot{V} = & \tilde{v}_y \left( -v_x \tilde{r} + K_{v_y} \sum_i [0 \ 1] \mathbf{R}(\delta_i) (\mathbf{F}_i - \hat{\mathbf{F}}_i) \right) + \\ & \tilde{r} \left( \frac{1}{J_z} \sum_i \mathbf{g}_i^T \mathbf{R}(\delta_i) (\mathbf{F}_i - \hat{\mathbf{F}}_i) - K_r \tilde{r} \right). \end{aligned}$$

By Lemma 1, this can be upper bounded:

$$\begin{aligned} \dot{V} \leq & -v_x \tilde{r} \tilde{v}_y - K_{v_y} c_1 \tilde{v}_y^2 + K_{v_y} c_2 |\tilde{r}| |\tilde{v}_y| \\ & + c_3 \tilde{r} |\tilde{v}_y| + c_4 \tilde{r} |\tilde{r}| - K_r \tilde{r}^2. \\ \leq & (v_x + K_{v_y} c_2 + c_3) |\tilde{r}| |\tilde{v}_y| - K_{v_y} c_1 \tilde{v}_y^2 + c_4 \tilde{r} |\tilde{r}| - K_r \tilde{r}^2. \end{aligned}$$

By Fact 1 and (9),

$$\begin{aligned} \dot{V} \leq & \frac{(v_x + K_{v_y} c_2 + c_3)^2}{2K_{v_y} c_1} \tilde{r}^2 - \frac{K_{v_y} c_1}{2} \tilde{v}_y^2 \\ & - \left( \sqrt{\frac{K_{v_y} c_1}{2}} |\tilde{v}_y| - \frac{(v_x + K_{v_y} c_2 + c_3)}{2\sqrt{\frac{K_{v_y} c_1}{2}}} |\tilde{r}| \right)^2 \\ & + c_4 \tilde{r} |\tilde{r}| - K_r \tilde{r}^2 \end{aligned}$$

We see that due to (10),

$$\dot{V} \leq -\frac{K_{v_y} c_1}{2} \tilde{v}_y^2 - k_r \tilde{r}^2 \quad (12)$$

is uniformly negative definite for  $\mathbf{x}, \hat{\mathbf{x}} \in X(\boldsymbol{\theta})$ .

By assumption,  $\mathbf{x}(t) \in X_s(\rho, \boldsymbol{\theta}(t)) \subset X(\boldsymbol{\theta}(t)) \forall t > 0$ , and we must show that  $\hat{\mathbf{x}}(t) \in X(\boldsymbol{\theta}(t)) \forall t > 0$ . Since  $\mathbf{x}(t) \in X_s(\rho; \boldsymbol{\theta})$  and  $\|\tilde{\mathbf{x}}(0)\| \leq \rho$ ,  $\hat{\mathbf{x}}(0) \in X(\boldsymbol{\theta}(0))$ . From the above,  $\frac{d}{dt} \|\tilde{\mathbf{x}}\| = \frac{\dot{V}}{\|\tilde{\mathbf{x}}\|} < 0$ , which means that  $\|\tilde{\mathbf{x}}(t)\| \leq \rho \forall t > 0$ , and thus  $\hat{\mathbf{x}}(t)$  will remain in  $X(\boldsymbol{\theta}(t))$ . Thus, from (12) and standard Lyapunov theory [15], we conclude that  $\tilde{\mathbf{x}}(t) \rightarrow 0$  with exponential convergence rate. ■

### C. Cascaded stability

Assuming that the longitudinal velocity estimate converges to its true value (that is, the slips are (eventually) zero), the following stability result hold on the overall system:

*Theorem 2:* Under the same conditions as in Theorem 1, there exists a set  $D \subset \mathbb{R}^3$  such that for initial observer error states in this set, the origin of the observer error dynamics is exponentially stable.

The proof follows from [15, Section 9.3] by treating the longitudinal velocity observer error as a vanishing perturbation to the lateral observer error dynamics, and is omitted for brevity.

As mentioned in Section IV-A, the presence of slips (and the neglected Coriolis term in the longitudinal dynamics) can be viewed upon as a time-varying, bounded disturbance to the longitudinal observer error dynamics. Similarly to

above, it can be shown that the cascaded system with this disturbance is uniformly ultimately bounded. This follows from [15, Lemma 9.4]. Again, the size of the ‘‘ultimate bounds’’ depends on the bound on the disturbance.

## V. DISCUSSION OF ASSUMPTION 2

This section discusses Assumption 2 for two friction models. Most friction models can be written as a function of (lateral and longitudinal) tyre slips  $\mathbf{F}_i = \mathbf{F}_i(\lambda_{i,x}, \lambda_{i,y})$  only, and depend thus on vehicle velocity only indirectly. Therefore, we can write the partial derivatives

$$\frac{\partial F_{i,x}}{\partial v_y} = \frac{\partial F_{i,x}}{\partial \lambda_{i,x}} \frac{\partial \lambda_{i,x}}{\partial v_y} + \frac{\partial F_{i,x}}{\partial \lambda_{i,y}} \frac{\partial \lambda_{i,y}}{\partial v_y} = \frac{\partial F_{i,x}}{\partial \lambda_{i,y}} \cos \alpha_i \frac{\partial \alpha_i}{\partial v_y} \quad (13)$$

$$\frac{\partial F_{i,y}}{\partial v_y} = \frac{\partial F_{i,y}}{\partial \lambda_{i,x}} \frac{\partial \lambda_{i,x}}{\partial v_y} + \frac{\partial F_{i,y}}{\partial \lambda_{i,y}} \frac{\partial \lambda_{i,y}}{\partial v_y} = \frac{\partial F_{i,y}}{\partial \lambda_{i,y}} \cos \alpha_i \frac{\partial \alpha_i}{\partial v_y} \quad (14)$$

where we have assumed  $\frac{\partial \lambda_{i,x}}{\partial v_y} = 0$ . Since

$$\frac{\partial \alpha_i}{\partial v_y} = \frac{-1}{1 + \tan^2(\delta_i - \alpha_i)} \quad (15)$$

is always negative, we see that it is the lateral slip partial derivatives that are significant (assuming  $|\alpha_i| < \pi/2$ ).

### A. Linear friction models

‘‘Linear’’ friction models says that the friction forces are proportional to the slips,

$$\begin{pmatrix} F_{i,x}(\mathbf{x}, \boldsymbol{\theta}) \\ F_{i,y}(\mathbf{x}, \boldsymbol{\theta}) \end{pmatrix} = \begin{pmatrix} C_x \lambda_{i,x} \\ C_y \lambda_{i,y} \end{pmatrix}$$

where  $C_x$  and  $C_y$  are tyre stiffness coefficients. In this case, Assumption 2 holds with

$$\Theta = \{\boldsymbol{\theta} : |\delta_i| \leq \bar{\delta}, v_x > \bar{r} b_i, i = 1, \dots, 4\},$$

$$X(\boldsymbol{\theta}) = \{\mathbf{x} = (v_y, r)^T : |\alpha_i| \leq \bar{\alpha}, |r| \leq \bar{r}, i = 1, \dots, 4\}.$$

### B. The magic formula tyre model

The ‘‘magic formula tyre model’’ [16] is a widely used semi-empirical model for calculating steady-state tyre forces. The ‘‘combined slip’’ magic formula provides similar formulas for lateral and longitudinal tyre forces<sup>1</sup>,

$$\begin{aligned} F_x(\lambda_x, \lambda_y) &= G_x(\lambda_y) F_{x0}(\lambda_x), \\ F_y(\lambda_x, \lambda_y) &= G_y(\lambda_x) F_{y0}(\lambda_y) \end{aligned}$$

where we have simplified somewhat since one of the parameters in  $G_x$  ( $G_y$ ) that according to [16] depends on  $\lambda_x$  ( $\lambda_y$ ) is assumed constant. For notational convenience we drop the dependence on wheel index  $i$  in this section.

The functions  $F_{x0}$  and  $F_{y0}$  are the ‘‘pure slip’’ formulas,

$$F_{x0}(\lambda_x) = D_x \sin \zeta_x, \quad F_{y0}(\lambda_y) = D_y \sin \zeta_y$$

where

$$\begin{aligned} \zeta_x &= C_x \arctan\{B_x \lambda_x - E_x(B_x \lambda_x - \arctan B_x \lambda_x)\} \\ \zeta_y &= C_y \arctan\{B_y \lambda_y - E_y(B_y \lambda_y - \arctan B_y \lambda_y)\}. \end{aligned}$$

<sup>1</sup>We use  $\lambda_y = \sin \alpha$  instead of  $\tan \alpha$  as in [16], but this is not significant for the conclusions drawn here.

The functions  $G_x$  and  $G_y$  are defined as  $G_x(\lambda_y) = \cos \eta_x$  and  $G_y(\lambda_x) = \cos \eta_y$  where

$$\eta_x = C_{G_x} \arctan\{B_{G_x} \lambda_y - E_{G_x}(B_{G_x} \lambda_y - \arctan B_{G_x} \lambda_y)\}$$

$$\eta_y = C_{G_y} \arctan\{B_{G_y} \lambda_x - E_{G_y}(B_{G_y} \lambda_x - \arctan B_{G_y} \lambda_x)\}.$$

We then have that

$$\frac{\partial F_y}{\partial \lambda_y} = G_y(\lambda_x) \frac{B_y C_y D_y \left(1 - E_y \left(1 - \frac{1}{1 + B_y^2 \lambda_y^2}\right)\right) \cos \zeta_y}{1 + \zeta_y^2}.$$

Since  $G(\lambda_x) > 0$  and  $E_y \leq 1$  [16, p. 189],  $\frac{\partial F_y}{\partial \lambda_y} > 0$  as long as  $|\zeta_y| < \pi/2$ . For “shape factor”  $C_y < 1$ , this holds for all  $\lambda_y$ . For  $C_y > 1$ , the friction force declines for large  $\lambda_y$ s, and  $\frac{\partial F_y}{\partial \lambda_y} > 0$  only to the left of the peak of the friction curve, that is, for  $|\lambda_y| \leq \bar{\lambda}$  where  $\bar{\lambda}$  is defined by

$$E_y = \frac{B_y \bar{\lambda} - \tan \frac{\pi}{2 C_y}}{B_y \bar{\lambda} - \arctan(B_y \bar{\lambda})}.$$

Furthermore,

$$\frac{\partial F_x}{\partial \lambda_x} = -F_{x0}(\lambda_x) \frac{B_{G_x} C_{G_x} \left(1 - E_{G_x} \left(1 - \frac{1}{1 + B_{G_x}^2 \lambda_x^2}\right)\right) \sin \eta_x}{1 + \eta_x^2}$$

We see that  $\text{sign} \frac{\partial F_x}{\partial \lambda_x} = -\text{sign}(\lambda_x \lambda_y)$  (since  $\text{sign} F_{x0}(\lambda_x) = \text{sign} \zeta_x = \text{sign} \lambda_x$  and  $\text{sign} \eta_x = \text{sign} \lambda_y$ ).

From the above, we make the following observations:

- For sufficiently small side-slip angles (that is,  $|\lambda_y| < \bar{\lambda}$ ) and small  $\delta$ , the first part of (3) is negative and dominates the second part.
- For  $\lambda_x \approx 0$  the second part of (3) is approximately zero, and hence dominated by the first part.
- For large side-slip angles, the first part of (3) will get less negative, and even positive if  $C_y > 1$ . However, in the case of braking ( $\lambda_x < 0$ ), then the second part of (3) will often contribute in fulfilling the assumption. Since  $\text{sign} \frac{\partial F_x}{\partial v_y} = \text{sign} \lambda_x \text{sign} \alpha$ , assuming that  $\text{sign} \alpha = \text{sign} \delta$ , gives  $\frac{\partial F_x}{\partial v_y} \sin \delta < 0$ .

In conclusion, (3) is negative for realistic slip values and sufficiently small steering angles for tyres with  $C_y < 1$ . For tyres with  $C_y > 1$ , then for some combinations of  $\lambda_x$  and (large)  $\lambda_y$ , it might be positive. Since it is the sum for all tyres that should be negative, a positive summand for one (or two) wheel(s) might be weighed against negative summands for the other wheels (for instance, rear wheels will often have lower side-slip angles due to small steering angle values). Finally, we remark that Assumption 2 is merely a (conservative) *sufficient* condition for stability.

## VI. EXPERIMENTAL RESULTS

The modular observer is applied to experimental data from a car. The velocity estimates ( $\hat{v}_x$ ,  $\hat{v}_y$  and side slip angle  $\hat{\beta} = \arctan(-\hat{v}_y/\hat{v}_x)$ ) are compared to velocity measurements obtained using an optical sensor placed in front of the vehicle.

The gains are chosen such that  $K_i(a_x)$  vary between 0 and 200 (but such that  $\sum_{i=0}^4 K_i(a_x) > 0$  always), and  $K_{v_y} = 1/m$  and  $K_r = 20$ . Notably, this particular choice of  $K_{v_y}$

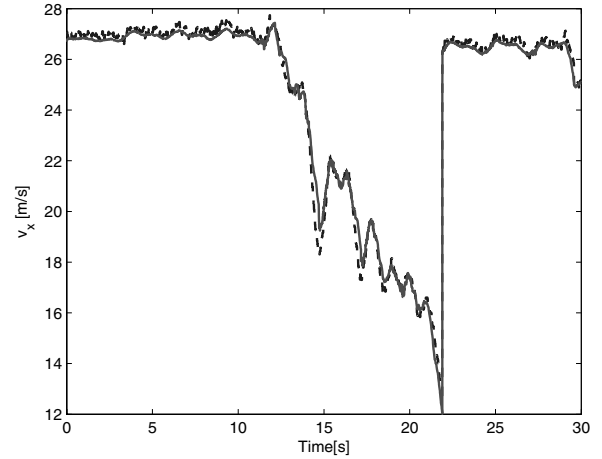


Fig. 3. Estimate (solid) and measurement (dashed) of longitudinal velocity, slalom maneuver.

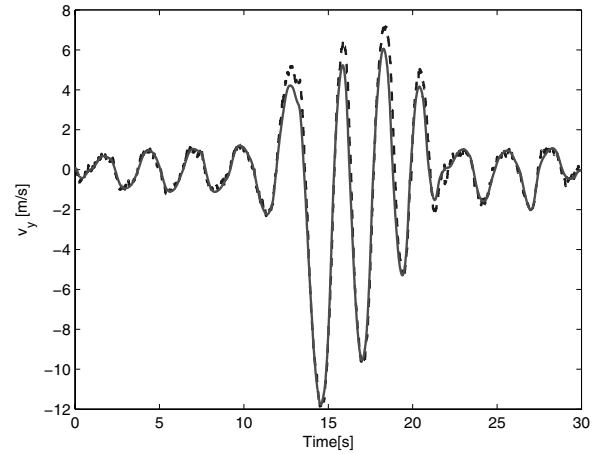


Fig. 4. Estimate (solid) and measurement (dashed) of lateral velocity, slalom maneuver.

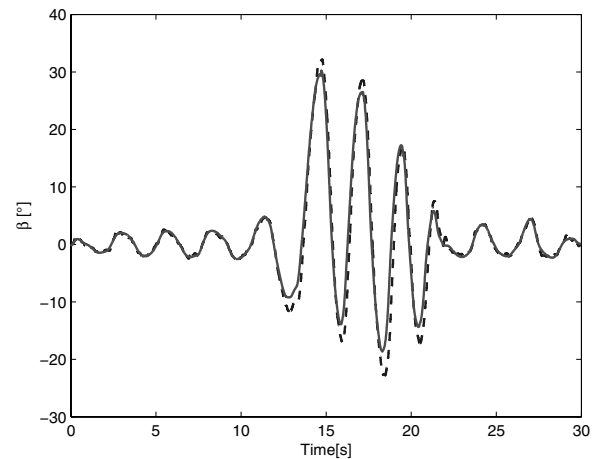


Fig. 5. Estimate (solid) and measurement (dashed) of side slip, slalom maneuver.

makes  $\hat{v}_y$  independent of  $a_y$ , hence implying fault tolerance and robustness to noise in this measurement.

Initial conditions for the observers are one of the wheel

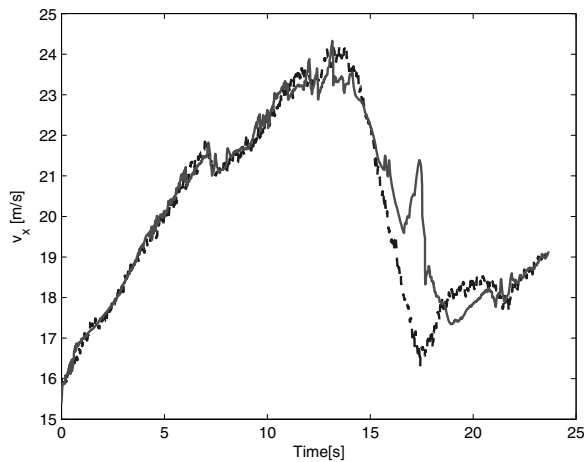


Fig. 6. Estimate (solid) and measurement (dashed) of longitudinal velocity, circle on ice.

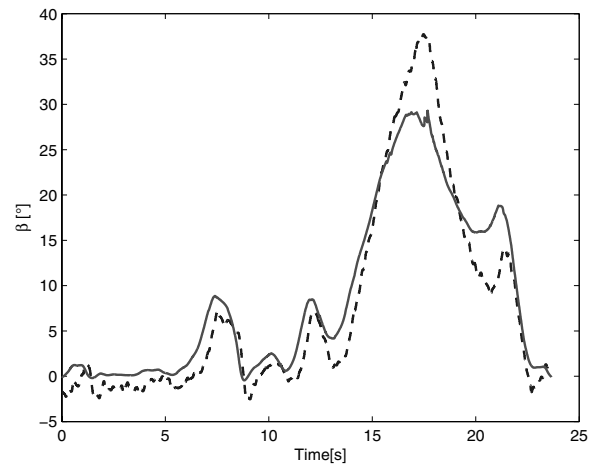


Fig. 8. Estimate (solid) and measurement (dashed) of side slip, circle on ice.

speeds (transformed to CG) for  $\hat{v}_x$ , and 0 for  $\hat{v}_y$  and  $\hat{r}$ . Experimenting with the initial conditions indicate a large region of attraction for reasonable maximum friction coefficient  $\mu_H$ .

1) *Flat dry road, slalom maneuver*: The maximum friction coefficient used in the observer is set to  $\mu_H = 1$ . The longitudinal velocity is shown in Fig. 3, while lateral velocity is shown in Fig. 4. The quality of both estimates are fine, so the vehicle side slip estimate, shown in Fig. 5, is also good.

2) *Ice, driving in circle*: The maximum friction coefficient used in the observer is set to  $\mu_H = 0.3$ . The longitudinal velocity is shown in Fig. 6. The estimate is rather inaccurate between 16.5s-17.5s. In this period, the wheel speed measurements are not used, and due to large lateral velocity, the Coriolis term (neglected herein) dominates the longitudinal acceleration. Work in progress address this shortcoming, as well as estimation of maximal friction coefficient.

The lateral velocity and side slip estimates are acceptable (Fig. 7 and 8). Reasons for lower quality estimates in this experiment are a less accurate friction model and varying friction coefficient, combined with larger slip values. Furthermore, driving in circle is a more difficult maneuver to estimate.

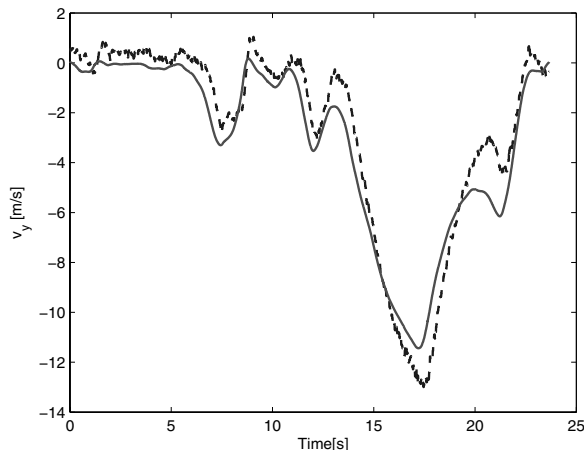


Fig. 7. Estimate (solid) and measurement (dashed) of lateral velocity, circle on ice.

## VII. CONCLUSION

A nonlinear observer for vehicle velocity and side-slip was proposed, with exponential stability of the observer error dynamics. The observer performs well when applied to experimental data from a car. Compared to an extended Kalman filter, the simple structure of the observer simplifies tuning considerably, and the real-time computational complexity is significantly reduced as real-time solution of the Riccati equation is avoided.

## REFERENCES

- [1] Y. Fukada, "Slip-angle estimation for stability control," *Vehicle Systems Dynamics*, vol. 32, pp. 375–388, 1999.
- [2] P. J. T. Venhovens and K. Nab, "Vehicle dynamics estimation using Kalman filters," *Vehicle System Dynamics*, vol. 32, pp. 171–184, 1999.
- [3] A. Y. Ungoren and H. Peng, "A study on lateral speed estimation methods," *Int. J. Vehicle Autonomous Systems*, vol. 2, no. 1/2, pp. 126–144, 2004.
- [4] J. Farrelly and P. Wellstead, "Estimation of vehicle lateral velocity," in *Proc. 35th IEEE Conf. Decision Contr.*, 1996, pp. 552–557.
- [5] U. Kiencke and A. Daiss, "Observation of lateral vehicle dynamics," *Control Engineering Practice*, vol. 5, no. 8, pp. 1145–1150, 1997.
- [6] U. Kiencke and L. Nielsen, *Automotive Control Systems*. Springer, 2000.
- [7] M. Hiemer, A. von Vietinghoff, U. Kiencke, and T. Matsunaga, "Determination of vehicle body slip angle with non-linear observer strategies," in *Proc. SAE World Congress*, 2005.
- [8] A. T. van Zanten, "Bosch ESP system: 5 years of experience," in *Proc. Automotive Dynamics & Stability Conference (P-354)*, 2000.
- [9] L. R. Ray, "Nonlinear state and tire force estimation for advanced vehicle control," *IEEE Transactions on Control Systems Technology*, vol. 3, no. 1, pp. 117–124, 1995.
- [10] —, "Nonlinear tire force estimation and road friction identification: simulation and experiments," *Automatica*, vol. 33, no. 10, pp. 1819–1833, 1997.
- [11] A. Suissa, Z. Zomotor, and F. Böttiger, "Method for determining variables characterizing vehicle handling," 1996, patent US 5557520.
- [12] M. C. Best, T. J. Gordon, and P. J. Dixon, "An extended adaptive Kalman filter for real-time state estimation of vehicle handling dynamics," *Vehicle System Dynamics*, vol. 34, pp. 57–75, 2000.
- [13] J. Lu and T. A. Brown, "Vehicle side slip angle estimation using dynamic blending and considering vehicle attitude information," 2003, patent US 6671595.
- [14] A. Hac and M. D. Simpson, "Estimation of vehicle side slip angle and yaw rate," in *SAE 2000 World Congress*, Detroit, MI, USA, 2000.
- [15] H. K. Khalil, *Nonlinear Systems*, 3rd ed. Upper Saddle River, NJ: Prentice Hall, 2002.
- [16] H. B. Pacejka, *Tyre and vehicle dynamics*. Butterworth-Heinemann, 2002.